Journal of Power Sources 221 (2013) 372–380

Contents lists available at SciVerse ScienceDirect

Journal of Power Sources

journal homepage: www.elsevier.com/locate/jpowsour

Hybrid solar–fuel cell combined heat and power systems for residential applications: Energy and exergy analyses

Mehdi Hosseini*, Ibrahim Dincer, Marc A. Rosen

Faculty of Engineering and Applied Science, University of Ontario Institute of Technology, 2000 Simcoe St. North, Oshawa, ON L1H 7K4, Canada

HIGHLIGHTS

- A residential solar PV–hydrogen CHP system is developed.
- The residential CHP system is assessed based on energy and exergy.
- The PV delivers its max. power to a house with 3.35 kW max. power demand.
- 0.792 kg hydrogen is generated with the surplus electricity of the PV.
- Maximum total energy and exergy efficiencies are 55.7% and 49%, respectively.

ARTICLE INFO

Article history:
Received 28 June 2012
Received in revised form
15 August 2012
Accepted 17 August 2012
Available online 24 August 2012

Keywords:
Photovoltaics
Hydrogen
Solid Oxide Fuel Cell
Combined heat and power
Exergy
Efficiency

ABSTRACT

Small-scale solar PV–water electrolyzer systems are suggested for remote combined heat and power (CHP) applications. A residential solar PV–electrolyzer system is developed and coupled with a high temperature solid oxide fuel cell (SOFC) system (PV–FC) for supplying the electricity demand. It is possible for the PV system to generate electricity in excess of the demand during off-peak hours. The surplus electricity is used by the water electrolyzer for hydrogen production. The hydrogen produced is stored in a storage tank. The fuel cell is fed with the hydrogen generated by the electrolyzer. The PV–FC system is coupled with a heat recovery unit, which provides the residential area with thermal energy, to improve energy utilization. The heat recovery unit consists of a heat recovery steam generator and an absorption chiller utilizing the thermal energy of the SOFC flue gas for heating and cooling purposes. Determining system operational parameters is important for the design and implementation of the CHP system in a residential area. Therefore, the residential CHP system is assessed here based on energy and exergy. The hourly demand of the residential area is taken into consideration for component selection and sizing, and energy and exergy efficiencies of the developed system are presented.

1. Introduction

Solar energy can be used for electricity generation with photovoltaic (PV) systems. Such systems normally require supplementary devices to meet peak demands or to harvest surplus electricity generation. Producing the energy carrier hydrogen is one method for storing electricity from solar PV systems. Surplus electricity can be converted to hydrogen via water electrolysis, and the hydrogen can be stored and used to generate electricity in a fuel cell when required. The fuel cell also can cogenerate heat for district heating or other purposes. In a hybrid PV–fuel cell combined heat and power (CHP) system, both electricity and heat are generated from solar energy.

Lu and Yang [1] report the results of the economic and environmental analysis of a rooftop building integrated renewable energy system in Hong Kong. That system consists of 126 monocrystalline PV cells in series and parallel. The PV system is connected to the local grid and the annual power output is 28,154 kWh. Lu and Yang report the energy payback period and greenhouse gas payback period as 7.3 and 5.2 years, respectively. Also, the results show that the installation orientation and location affect the sustainability of the PV system.

Uzunoglu et al. [2] propose an integrated system to meet the power demand of a building. A solar PV system is integrated with a water electrolyzer, an ultra-capacitor bank and a fuel cell for sustained power generation. The hourly difference in the PV output and the load demand is calculated, along with the hydrogen production rate in the electrolyzer. The dynamic behaviour of the hybrid system is tested under varying solar radiation and load

* Corresponding author. Tel./fax: +1 905 721 8668.
E-mail addresses: mehdi.hosseini@uoit.ca, mehdi.m.hosseini@gmail.com (M. Hosseini).

0378-7753/$ – see front matter © 2012 Elsevier B.V. All rights reserved.
http://dx.doi.org/10.1016/j.jpowsour.2012.08.047

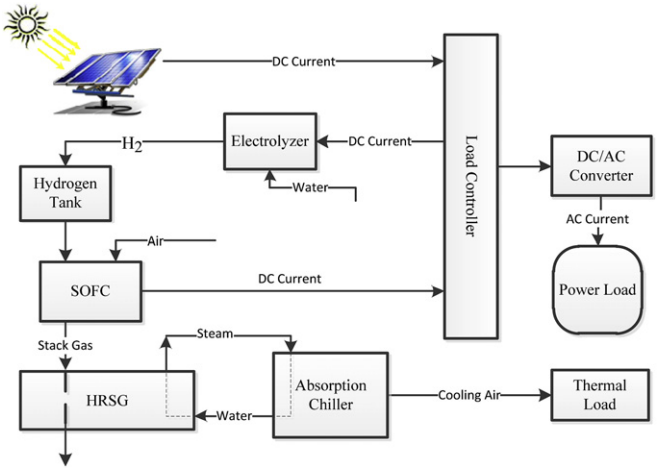

Fig. 1. Schematic of the photovoltaic–fuel cell CHP system for residential applications.

demand conditions where the solar radiation and power demand data are based on real-world data.

Direct coupling of electrolyzers to solar PV systems for hydrogen production is studied by Clarke et al. [3]. Direct coupling eliminates most of the interfacing electronic systems; therefore, the cost of the PV–electrolyzer system is reduced. The experimental set-up follows the maximum power generated by the PV system, which is directly introduced to the electrolyzer. The efficiency of the PEM electrolyzer is affected by cell degradation due to repetitive variations of the load, and an overall electrolyzer stack efficiency of 65% is reported.

Solar PV–hydrogen systems can also be integrated with Solid Oxide Fuel Cells (SOFCs), due to their high efficiency and capability as distributed power generators. Hawkes et al. [4] consider using an SOFC as the power and heat generator of a residential area in the United Kingdom. Different thermal demand profiles are considered, along with the environmental and economic investigation of the combined heat and power systems. The results show that the system has its best performance for slow steady thermal demand. Numerous integration strategies for SOFCs are reviewed by Zhang et al. [5]. They conclude that integrated SOFC systems have higher efficiencies and lower environmental loads. Reversible solid oxide fuel cells integrated with solar PV power generation systems are said to be a promising substitute for solar PV-battery systems. In these systems, a reversible SOFC acts as the electrolyzer for hydrogen generation, when excess electricity from the PV system is available. It also operates as a power generation system when the PV power is unavailable.

Moreover, the Canadian Centre for Housing Technology tested a solid oxide fuel cell in a combined heat and power system for residential applications. The CHP system was operated for 1587 h and provided the house with both electricity and cooling with a total efficiency of 52% [6]. Heat recovery from the gases leaving a solid oxide fuel cell stack is studied by Hosseini et al. [7,8]. The SOFC stack gas is directed to a heat recovery steam generator (HRSG) for steam generation. The steam generated can be utilized for different purposes. Hosseini and Ziabasharhagh [8] propose utilizing the generated steam in an absorption chiller to supply the cooling demand of a residential area.

Load variation and changes in weather conditions affect the performance of solar PV–hydrogen systems. Sudden load variations result in component degradation and reduce the lifetime of the system. Tesfahunegn et al. [9] proposed the use of an existing peak shaving battery to suppress short-term PV and load fluctuations. This enables the fuel cell and electrolyzer to operate under more favorable power conditions, which improve performance and lifetime.

Some other solar PV–hydrogen systems and their integration with fuel cell systems have been reported [10,11]. PV characteristic curves, power output and hourly hydrogen production are the main focus of these works. The fuel cell behaviour and the payback time are also concerns. However, these integrated systems need to be analyzed from a thermodynamic point of view to understand their efficiencies and effectiveness, based on both energy and exergy.

Therefore, the main objective of the present work is to perform energy and exergy analyses of a residential PV–fuel cell CHP system. Gaseous hydrogen storage is considered as the energy storage option. The hourly behaviour of the system is examined to determine the hydrogen production rate and the overall efficiencies of the hybrid system.

2. System description

The solar PV system is the main part of the electricity generation module. A PEM water electrolyzer is utilized for hydrogen

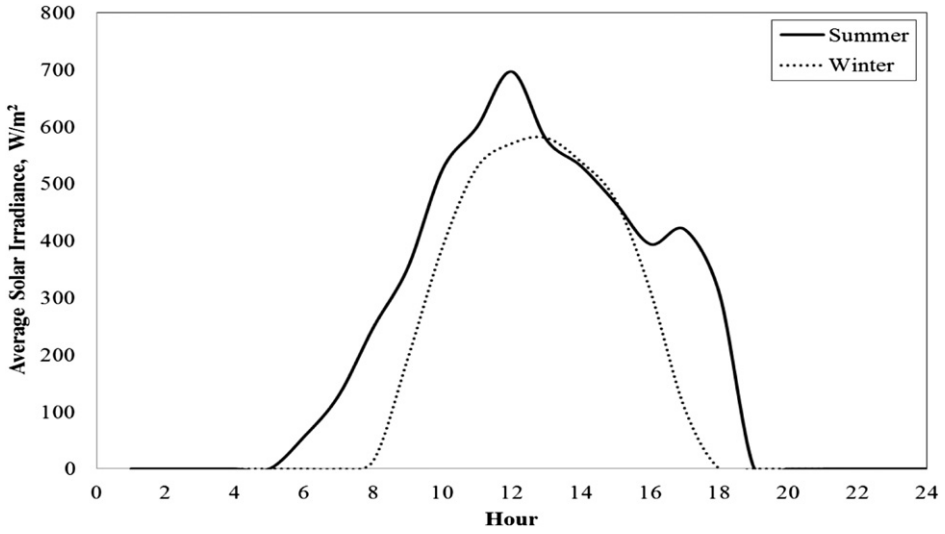

Fig. 2. Hourly solar irradiance broken down by hour of the day [20].

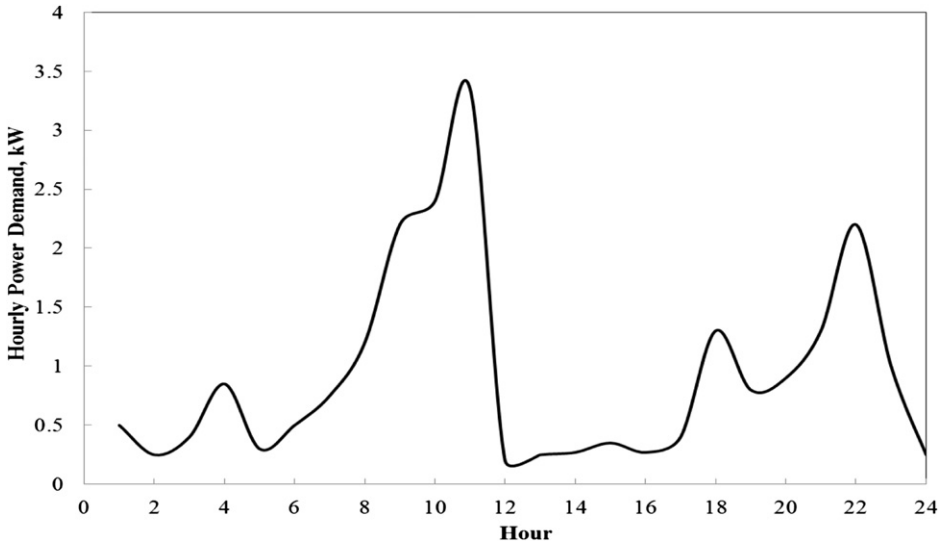

Fig. 3. Hourly electric power demand of the apartments broken down by hour of the day.

production from surplus PV electricity. Hydrogen is stored during day when loads are below the peak and input to the SOFC to provide residential electricity at night.

An atmospheric SOFC is used in the modeling, so the hydrogen temperature rises when its pressure decreases from the storage tank pressure (5 bar) to atmospheric pressure (1 bar). If preheating is still required, an external heat source is considered for this purpose, however, only the amount of the required heat is calculated in the analysis.

High temperature gases leaving the stack are directed to a heat recovery steam generator (HRSG), as shown in Fig. 1, for steam generation. The HRSG provides steam for an absorption chiller, which operates based on a lithium-bromide refrigeration cycle. The HRSG and the absorption chiller operate only when the SOFC is in operation. The PV and SOFC power output are converted in a DC/AC converter to meet the power requirements of the house.

3. Analysis

3.1. Photovoltaic system

PV systems are combinations of series and parallel cells producing desired current and voltage outputs. The performance of these systems exhibits non-linear current–voltage (I–V) characteristic curves. Masoum et al. [12], Veerachary et al. [13], and Chenni et al. [14] present comprehensive models of PV systems. They express the I–V characteristic as

$$I = I_L - I_0\left[\exp\left(\frac{q(V+IR_s)}{\gamma k T_{cell}}\right) - 1\right] \quad (1)$$

The light current (I_L) depends on solar irradiance and temperature [14]:

$$I_L = \left(\frac{G}{G_{ref}}\right)\left(I_{L,ref} + k_t\left(T_{cell} - T_{ref}\right)\right) \quad (2)$$

where G is solar insolation (W m^{-2}), G_{ref} is the solar insolation at the design condition, $I_{L,ref}$ is calculated based on the manufacturer data for short-circuit and maximum point currents, and k_t is the manufacturer supplied temperature coefficient of short-circuit current (A °C^{-1}).

The PV system performance is affected by the ambient temperature, and is considered in the modeling through Eq. (2), in which the cell temperature is a function of the ambient temperature. Wind speed also affects the cell temperature and is accounted for in the modeling (see Eq. (3)). The PV cell temperature is determined by Eq. (3), as a function of ambient temperature, wind speed, and total irradiance [14]:

$$T_{cell} = 0.943T_0 + 0.028G - 1.528V_{wind} + 4.3 \quad (3)$$

where V_{wind} is the wind speed in m s^{-1}.

Note that in Eq. (1), I_0 is the reverse saturation current which is a function of the cell temperature, material band gap energy (1.12 eV for silicon cells). The value of I_0 is very small and is in the order of 10^{-5} A [14]. The shape factor in Eq. (1), γ is a measure of cell imperfection and is related to the completion factor as follows:

$$\gamma = a \times NS \times NCS \quad (4)$$

where NCS is the number of cells connected in series in each module, and NS is number of modules connected in series.

The PV cell power output is $I \times V$ and based on the non-linear characteristic of Eq. (1), there is a point at which the maximum power output is obtained. The corresponding current and voltage values are called I_{mp} and V_{mp}, and the subsequent power output is P_{mp}. The control system for the PV system is designed so that the system operates at the maximum power point.

Table 1
PV module specifications.[a]

Short-circuit current, I_{sc} (A)	5.75
Open-circuit voltage, V_{oc} (V)	47.7
Maximum point current, I_{mp} (A)	5.25
Maximum point voltage, V_{mp} (V)	40
Array area (m^2)	1.244
Number of cells in module, NCS	72
Number of modules in series, NS	7
Number of modules in parallel, NP	7
Temperature coefficient of short-circuit current (A °C^{-1})	3.5×10^{-3}
Temperature coefficient of open-circuit voltage (V °C^{-1})	-1.36×10^{-1}
Reference conditions	
Total irradiance, G_{ref} (m^{-2})	1000
Wind speed (m s^{-1})	5
Ambient temperature, T_a (°C)	25

[a] Adapted from [18].

Table 2
Input parameters to the SOFC model.

Inlet air temperature (°C)	25
Stack temperature (°C)	900
Activation area (cm^2)	834 [15]
Cell current density (A cm^{-2})	0.3
Fuel utilization	0.85 [15]
Number of cells	15

The energy and exergy efficiencies of the photovoltaic system can be shown to be

$$\eta_{PV} = \frac{P_{PV}}{\dot{E}n_{solar}} = \frac{I \times V}{G \times A_{cell}} \tag{5}$$

$$\psi_{PV} = \frac{P_{PV}}{\dot{E}x_{solar}} = \frac{I \times V}{G \times A_{cell} \times \left(1 - \frac{4}{3}\frac{T_0}{T_{sun}} + \frac{1}{3}\left(\frac{T_0}{T_{sun}}\right)^4\right)} \tag{6}$$

The energy and exergy efficiencies of the PV cell at maximum power point are given by

$$\eta_{PV,mp} = \frac{P_{mp}}{\dot{E}n_{solar}} = \frac{I_{mp} \times V_{mp}}{G \times A_{cell}} \tag{7}$$

$$\psi_{Pv,mp} = \frac{P_{mp}}{\dot{E}x_{solar}} = \frac{I_{mp} \times V_{mp}}{G \times A_{cell} \times \left(1 - \frac{4}{3}\frac{T_0}{T_{sun}} + \frac{1}{3}\left(\frac{T_0}{T_{sun}}\right)^4\right)} \tag{8}$$

3.2. Water electrolyzer

For surplus electricity of the PV system, $P_{in,el}$, the energy efficiency relation of the electrolyzer is used to calculate the produced hydrogen flow rate:

$$\eta_{el} = \frac{\dot{m}_{H_2} LHV_{H_2}}{P_{in,el}} \tag{9}$$

3.3. Solid oxide fuel cell

The SOFC in this study is based on a tubular design, with geometric and material related data as given by Motahar and Alemrajabi [15]. The fuel cell hydrogen consumption and power output are calculated based on the model developed by Dincer et al. [16].

The SOFC is fed by hydrogen and serves as the power source when power demand is higher than the PV output power. The produced hydrogen then undergoes an anodic, electrochemical oxidation reaction with oxygen ions from the cathode. The hydrogen consumption rate is related to the current density in the fuel cell. The net electric power output of the fuel cell is given is

$$\dot{W}_{net-SOFC} = \dot{W}_{SOFC} - \dot{W}_{FWP} - \dot{W}_{consumption} \tag{10}$$

where $\dot{W}_{FWP}$ denotes the feed water pump power consumption of the HRSG, and $\dot{W}_{consumption}$ accounts for the internal consumption of the fuel cell system, e.g. air blower, control system, etc. The energy and exergy efficiencies for the fuel cell are

$$\eta_{SOFC} = \frac{\dot{W}_{net-SOFC}}{\dot{m}_{H_2,SOFC}\, LHV_{H_2}} \tag{11}$$

$$\psi_{SOFC} = \frac{\dot{W}_{net-SOFC}}{\dot{m}_{H_2,SOFC}\, ex_{H_2}} \tag{12}$$

The gases exiting the SOFC anode undergo a combustion reaction in the afterburner with the non-reacted oxygen from the cathode. The combustion gases are fed to the HRSG to produce steam for the absorption chiller. The cooling thermal load provided by the chiller helps improve the fuel utilization in the CHP system. The efficiency of the SOFC-chiller system is

$$\eta_{SOFC-CH} = \frac{\dot{W}_{SOFC} + \dot{Q}_{evap}}{\dot{m}_{fuel}\, LHV} \tag{13}$$

$$\psi_{SOFC-CH} = \frac{\dot{W}_{SOFC} + \dot{Q}_{evap}\left(1 - T_0/T_{evap}\right)}{\dot{m}_{fuel}\, ex_{H_2}} \tag{14}$$

where $\dot{m}_{fuel}$ is the total hydrogen consumption rate in the fuel cell and the afterburner.

The purpose of this renewable energy CHP system is to provide the residential area with zero-emission electric and thermal energy. The hourly based total efficiency of the PV–fuel cell CHP system is defined accordingly. Therefore, the total efficiencies are

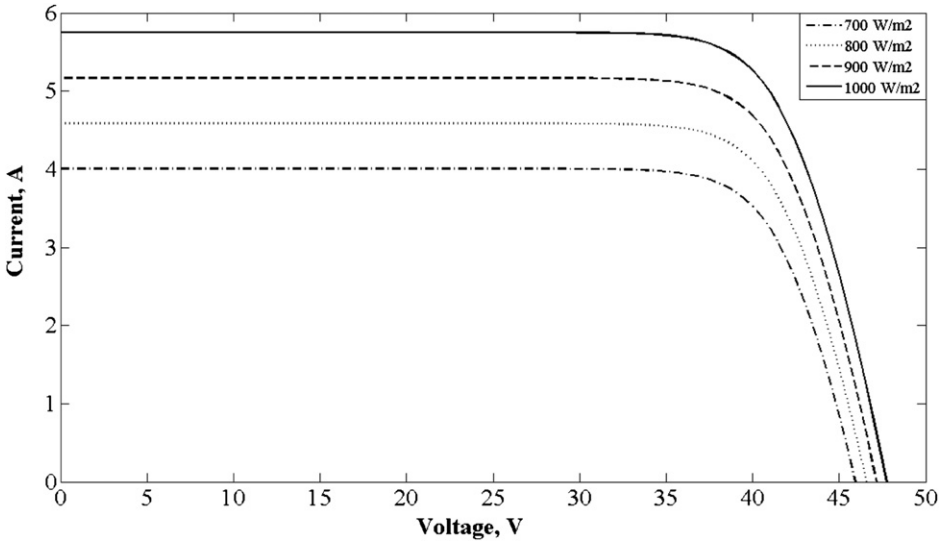

Fig. 4. Effect of solar irradiance on *I–V* characteristics.

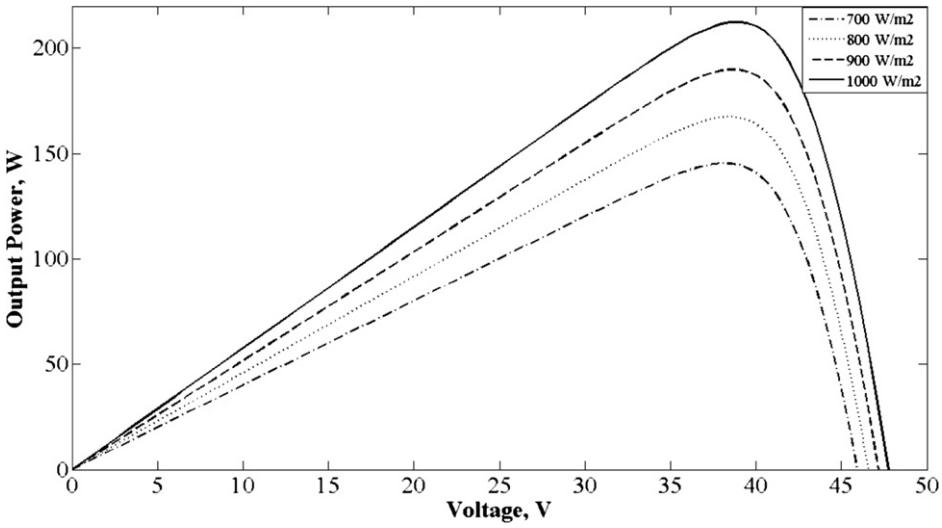

Fig. 5. Effect of solar irradiance on power–voltage characteristics.

different for each time step, depending on the operation of the system.

If the PV system is in operation and the power surplus is directed to the electrolyzer for hydrogen production, the total efficiencies are calculated as follows:

$$\eta_{\text{total}} = \frac{P_{\text{demand}} + \dot{m}_{\text{H}_2}\text{LHV}}{\dot{E}n_{\text{solar}}} \tag{15}$$

$$\psi_{\text{total}} = \frac{P_{\text{demand}} + \dot{m}_{\text{H}_2} ex_{\text{H}_2}}{\dot{E}x_{\text{solar}}} \tag{16}$$

For the hours that the PV is not in operation and the SOFC provides electricity for the residential area, the total efficiencies are the same as in Eqs. (13) and (14).

4. Assumptions and data

The following assumptions are made in the analyses:

- The hybrid system operates at steady-state.
- The data for solar irradiance, as well as the load variations, are for 1 h time periods.
- Possible sources of data noise, e.g. sudden changes in solar irradiance and electric power demand, are not considered in the analyses (i.e. average values are used).
- The electric load profile is based on the data in Fig. 3, which is used as a sample profile to perform the analyses.
- The PV panels are well maintained, so their performance is not affected by dust accumulation.
- The PV modules are facing south, and are tilted at the optimum 28° angle from horizontal in summer days for Toronto, ON [17].
- Heat losses from the system boundary are negligible.

Here, c-Si photovoltaic modules manufactured by SunPower Corporation, with specifications shown in Table 1, are selected for analysis. The SOFC electrolyte is made of Y_2O_3-Stabilized Zirconia (YSZ), the anode material is YSZ with a coating of Nickel, and the cathode is made of Sr-doped $LaMnO_3$ (LSM) + YSZ [19]. The major input parameters to the SOFC are presented in Table 2. The internal

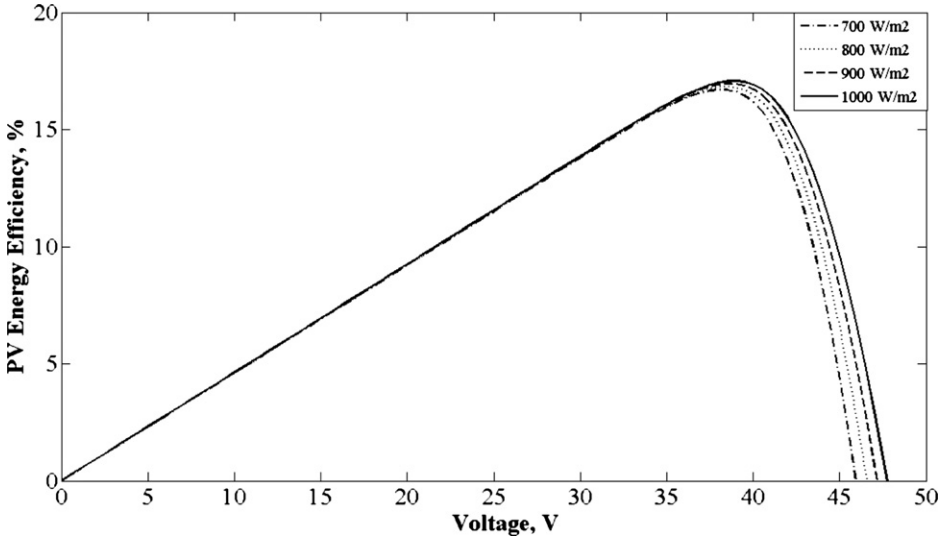

Fig. 6. PV energy efficiency vs. voltage with various solar irradiance.

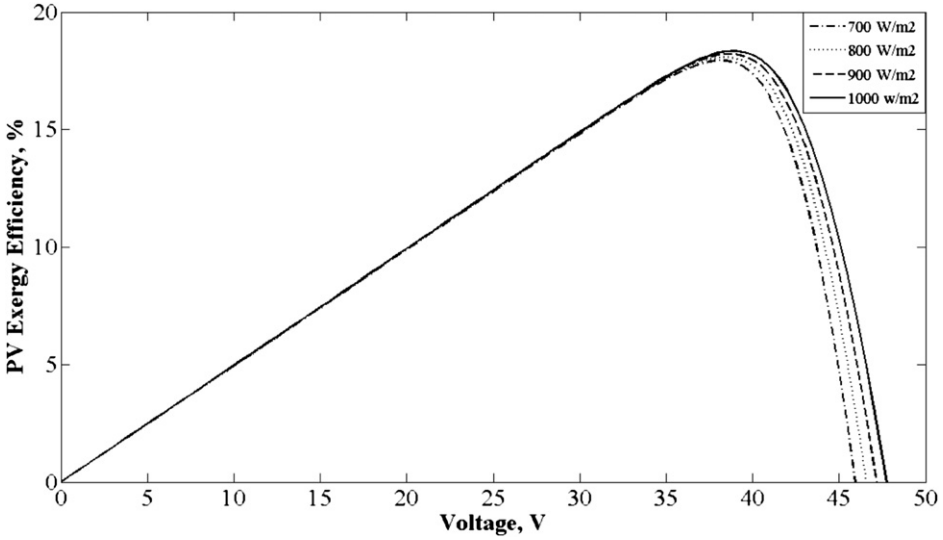

Fig. 7. PV exergy efficiency vs. voltage with various solar irradiance.

consumption of the SOFC balance of plant is considered to be 4% of the generated power, and this is accounted for in efficiency calculations. The efficiency of the DC/AC inverter is taken to be 96% [15].

The recorded data for solar irradiance in Toronto in Summer and Winter 2011 published by University of Toronto [20] are used in the analysis. These two seasons are selected because of their extreme weather conditions comparing to Spring and Fall. Fig. 2 shows the average daily solar irradiance. The averaged data for the summer of 2011 shows that between 9 pm and 5 am, the solar irradiance is zero. Solar unavailability for the winter of 2011 is from 6 pm to 8 am. During these periods, the power output of the photovoltaic system is zero. The PV power is highly dependent on the solar radiation, so the maximum power is generated by the PV system between 11 am and 1 pm during summer and 12 pm and 2 pm in winter. The total solar irradiance in summer 2011 is higher than the reported values for winter, according to Fig. 2. Correspondingly, the solar exergy is higher in the summer because of the higher intensity of the solar energy.

The analysis requires the selection of an electric load profile, which fits the Canadian household energy consumption. The electric power demand (Fig. 3) of a detached house with 140 m^2 floor area is considered and the load profile data are adapted from a report of Annex 42, by International Energy Agency [21]. Statistical tools are used to calculate the daily energy consumption of a Canadian family house, taking into account all electric appliances and devices. The presented data for daily load profile shows similar patterns for winter, summer and shoulder seasons in electricity consumption for lighting, except that the maximum demand begins at 6 pm in winter season comparing to 9 pm in summer time. Aside from this difference, the electricity consumption of the appliances has the same pattern throughout the year. The hourly average profile for the house is used in the present analysis of the PV–FC hybrid system.

A low temperature PEM electrolyzer is selected because its response time to load variations is shorter than for SOFCs. Therefore the PEM electrolyzer responds faster to load and solar availability variations due to changes in the solar irradiance (shading, cloudy sky, etc.). The efficiency of the electrolyzer is considered to be 65%, according to Clarke et al. [3]. They report direct coupling of a PEM electrolyzer to the PV system. Although they expect higher values,

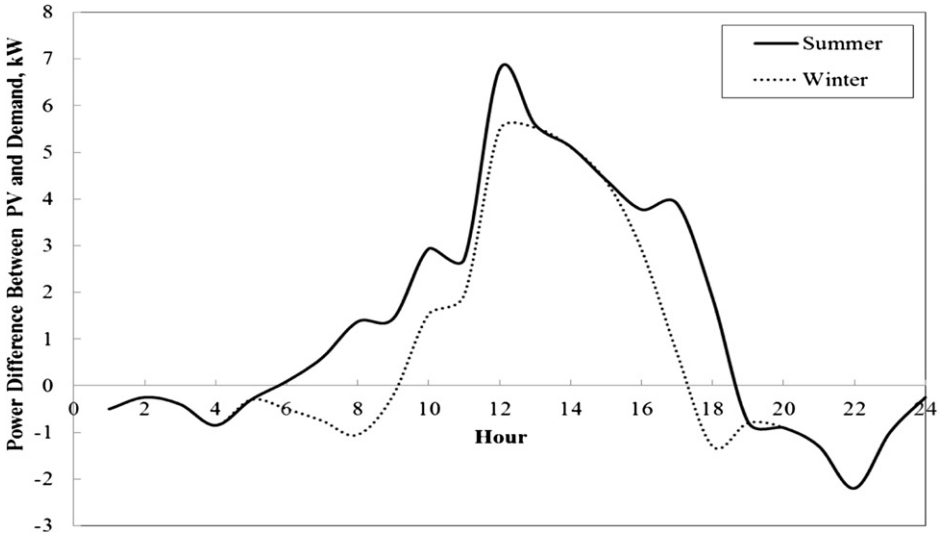

Fig. 8. Difference between the PV output and the demand power of the apartments broken down by hour of the day.

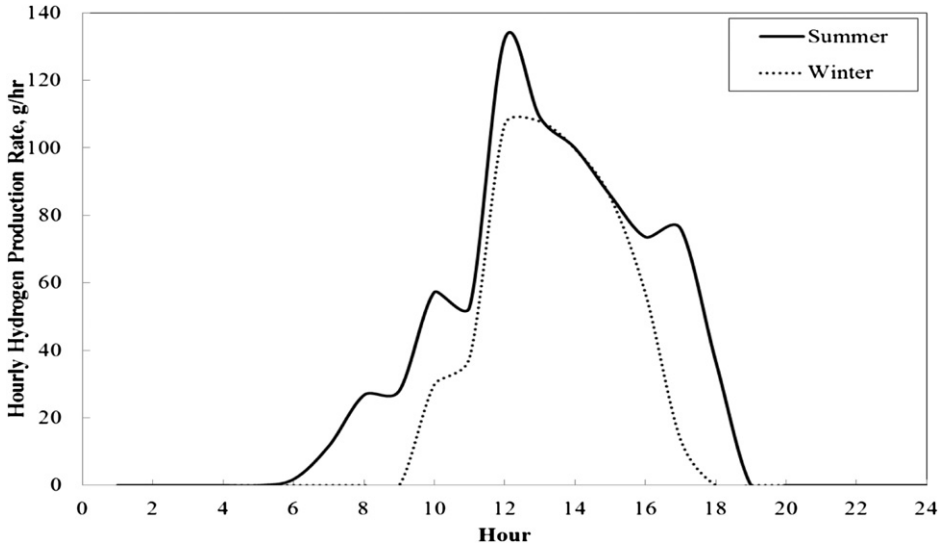

Fig. 9. Hydrogen production rate in the electrolyzer broken down by hour of the day.

the efficiency of the electrolyzer is less because of stack performance degradation.

5. Results and discussion

5.1. PV characteristics and efficiencies

Fig. 4 shows the *I–V* characteristic of the PV system for various values of solar irradiance. The system characteristic considerably deviates from the design condition as solar irradiance decreases. According to Fig. 5, the power output of the PV module has a maximum point, after which the power drops significantly. The novel PV systems are designed to operate at the maximum power point with the change in solar irradiance. The results of the PV model are compared to the SunPower 210 solar panel's *I–V* characteristic curves for the standard test condition (STC) irradiance 1000 W m^{-2}, and temperature 25 °C. The obtained maximum power point at STC is only 2.4% different from the manufacturer's reported value.

Figs. 6 and 7 show that the efficiencies of the PV system follow the same trend as the power output. Higher efficiencies are obtained for higher solar irradiances. The exergy efficiency at the maximum power output is higher than the corresponding energy efficiency. This can be explained by Eqs. (7) and (8). While the energy and exergy values of the PV electric power output are the same, the exergy of solar irradiance is less than its energy value. Since the latter term is present in the denominator of Eq. (8), the exergy efficiency is higher than the energy.

5.2. Hybrid CHP system performance

The average solar irradiance in Summer and Winter 2011 is used to analyze the hybrid CHP system, when determining electric power demand, hydrogen generation rate, and total system efficiencies. Fig. 8 shows the differences in electric power generated by the photovoltaic system and the power demand of the detached house. The nominal PV system size is the same for the both seasons; however, due to higher solar irradiance in Summer, the power

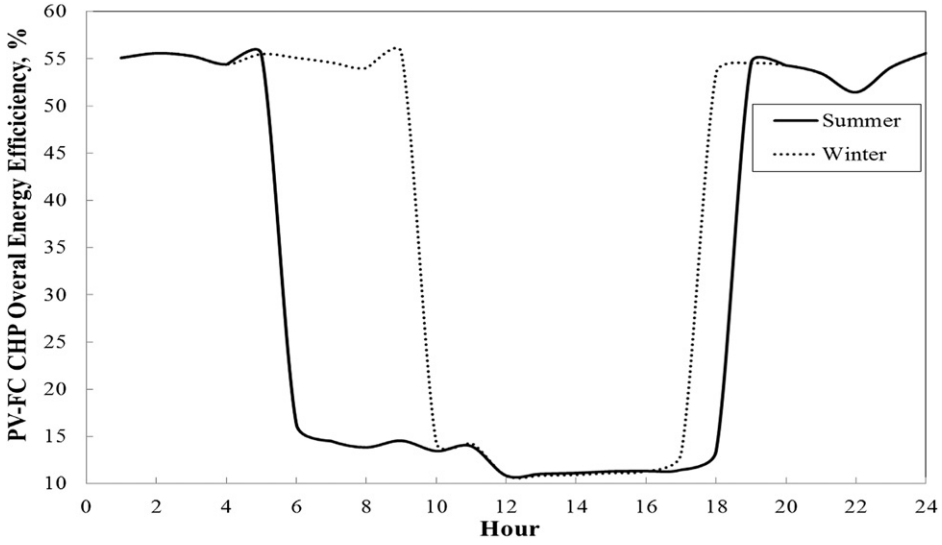

Fig. 10. Total energy efficiencies of the solar CHP system broken down by hour of the day.

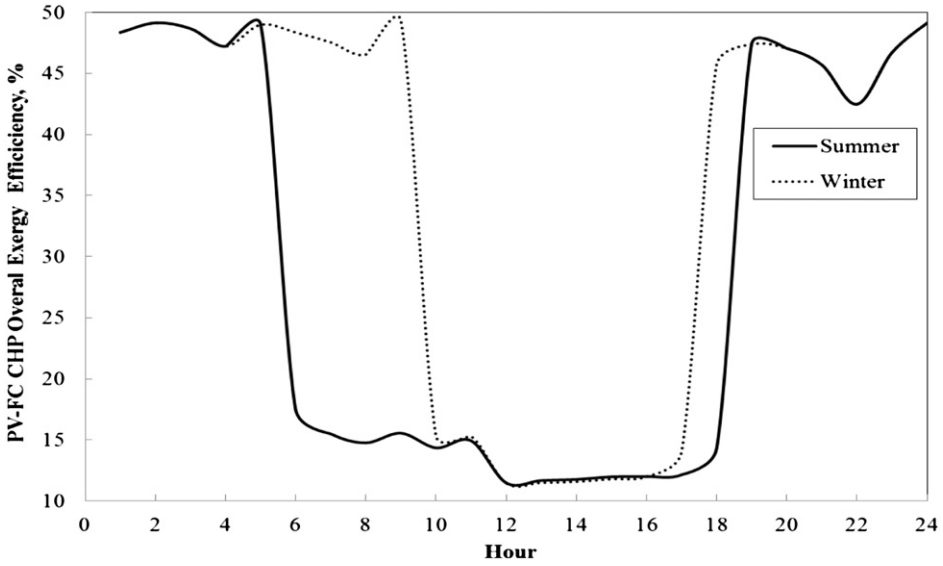

Fig. 11. Total exergy efficiencies of the solar CHP system broken down by hour of the day.

generated by the photovoltaic system is greater. This results in higher values for the difference in PV electric output and the power demand of the house. When the power difference is positive, the electrolyzer operates to generate hydrogen. With 65% energy efficiency of the electrolyzer, the hydrogen generation rate, on an hourly basis, is shown in Fig. 9. Obviously, more hydrogen is generated in Summer, which can be calculated as the surface area under the curves in Fig. 8. For the hours in which the power difference is negative, the fuel cell generates electricity to compensate for the power difference.

The total efficiencies of the renewable PV–fuel cell CHP system are calculated using Eqs. (13)–(16) and shown in Figs. 10 and 11. The energy efficiency is higher than the exergy efficiency because the exergy output of the chiller is lower than its energy value. The efficiencies have similar patterns for the seasons under study. The efficiency graphs show that the time that the fuel cell is in operation is longer in winter. This is mostly due to less solar availability in winter. The minimum total efficiency is achieved when surplus electricity generation is a maximum. In summer, the system exhibits minimum total energy and exergy efficiencies between 6 am and 6 pm, because the surplus power generated by the PV system is consumed in the electrolyzer for hydrogen production. This minimum efficiency operation period for winter is from 10 am to 5 pm. According to Fig. 6, the maximum energy efficiency of the PV system is 17%, which is for the case where the solar insolation is 1000 W m^{-2}. This means that only 17% of the solar energy received is converted to electric energy in the PV cells. Since the PV output is considerably higher than the power demand (Fig. 8) only a part of the generated electricity is consumed by the user. The surplus electricity is used for hydrogen production in the water electrolyzer, which has an energy efficiency of 65%. Therefore, the total output of the PV–hydrogen system between 6 am and 6 pm is the sum of energy provided to the apartments and the energy content of the generated hydrogen. During this time period, solar availability, which is the energy input to the PV–hydrogen system, is a maximum. The efficiencies of the system, according to Eqs. (15) and (16), are as reported in Figs. 10 and 11. However, converting the hydrogen stored back to electricity in the fuel cell boosts the

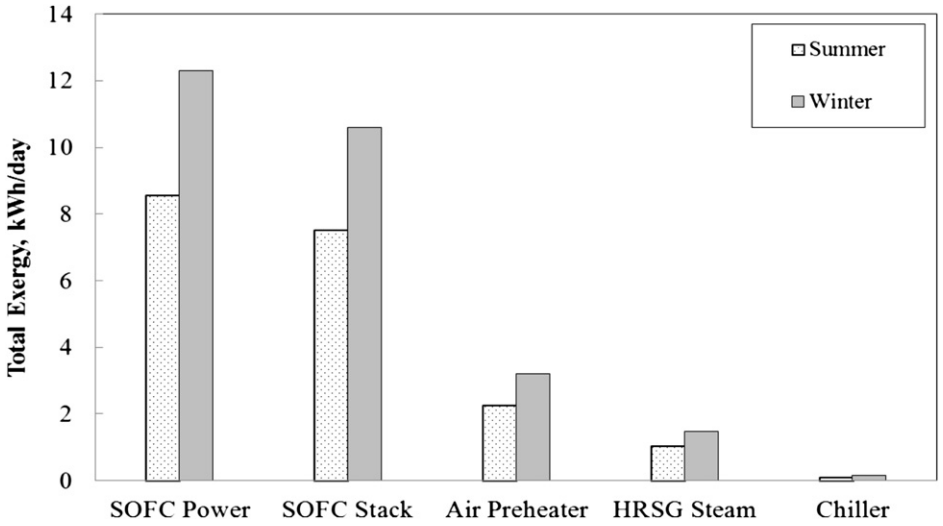

Fig. 12. Total daily exergy of the fuel cell CHP system.

total efficiency significantly. With the aid of the heat recovery system, the efficiency increase is more considerable.

The total daily electric power demand of the detached house is 22.3 kWh day^{-1}, of which the fuel cell provides 8.43 kWh day^{-1} based on the summer solar irradiance and 12.3 kWh day^{-1} in a winter day. The exergy contents of the fuel cell–CHP system are presented in Fig. 12. The SOFC stack gas has considerable exergy (7.90 kWh day^{-1} in summer and 11.1 kWh day^{-1} in winter). Most of this exergy is used to preheat the fuel cell inlet air. The remaining exergy (preheater outlet) is recovered in the HRSG, resulting in steam generation, as shown in Fig. 12. The steam generated in the HRSG can transfer its energy to the house hot water supply system directly, or it can be introduced to the absorption chiller for space cooling/heating purposes, depending on the season.

6. Conclusions

Hourly power generation by the photovoltaic system is studied and presented. The PV system is considered to deliver its maximum power output to a residential area with 3.35 kW maximum power demand (total 22.3 kWh day^{-1}). For the available solar irradiance in Toronto, 0.792 and 0.538 kg day^{-1} hydrogen are generated with the surplus electricity of the PV, in Summer and Winter 2011 respectively. The SOFC meets the power demand of the house during solar unavailability. The maximum energy and exergy efficiencies of the photovoltaic system are 17% and 18.3%, respectively. The total efficiency of the PV–fuel cell CHP system is related to the pattern of the power demand and solar availability. The maximum total energy efficiency is reported as 55.7%, while the maximum total exergy efficiency is 49.0%. These results are obtained for the hours that the fuel cell is in operation.

Acknowledgments

The authors acknowledge the support provided by the Natural Sciences and Engineering Research Council of Canada.

Nomenclature

a	completion factor
ex	specific exergy, kJ kg^{-1}
$\dot{E}n$	energy flow rate, kW
$\dot{E}x$	exergy flow rate, kW
G	solar irradiance, kW m^{-2}
I_L	PV light current, A
I_0	reverse saturation current, A
I	PV electric current, A
k	Boltzmann constant
k_t	manufacturer supplied temperature coefficient of short-circuit current, A °C^{-1}
LHV	lower heating value, kJ kg^{-1}
$\dot{m}$	mass flow rate, kg s^{-1}
P	power, kJ
$\dot{Q}$	heat transfer rate, kW
R_s	series resistance of the PV cells, Ohm
T	temperature, K
V	electric voltage, V
$\dot{W}$	work rate, kW

Greek letters

γ	PV cell shape factor
η	energy efficiency, %
ψ	exergy efficiency, %

Subscripts

0	ambient condition
cell	PV cells
evap	evaporator
FWP	feed water pump
H_2	hydrogen
in,el	input to the electrolyzer
mp	maximum power
SOFC	solid oxide fuel cell

Acronyms

CHP	combined heat and power
FWP	feed water pump
PV	photovoltaic
SOFC	Solid Oxide Fuel Cell
STC	standard test condition

References

[1] L. Lu, H.X. Yang, Appl. Energy 87 (2010) 3625–3631.
[2] M. Uzunoglu, O.C. Onar, M.S. Alam, Renew. Energy 34 (2009) 509–520.
[3] R.E. Clarke, S. Giddey, F.T. Ciacchi, S.P.S. Badwal, B. Paul, J. Andrews, Int. J. Hydrogen Energy 34 (2009) 2531–2542.
[4] A.D. Hawkes, P. Aguiar, B. Croxford, M.A. Leach, C.S. Adjiman, N.P. Brandon, J. Power Sources 164 (2007) 260–271.
[5] X. Zhang, S.H. Chan, G. Li, H.K. Ho, J. Li, Zh. Feng, J. Power Sources 195 (2010) 685–702.
[6] M. Bell, M.C. Swinton, E. Entchev, J. Gusdorf, W. Kalbfleisch, R. Marchand, F. Szadkowski, Canadian Center for Housing Technology (December 8, 2003). Report ID Number: B-6010.
[7] M. Hosseini, I. Dincer, H.B. Avval, P. Ahmadi, M. Ziabasharhagh, Int. J. Energy Res. (22 Nov. 2011). http://dx.doi.org/10.1002/er.1945.
[8] M. Hosseini, M. Ziabasharhagh, ECOS 2010 Proceedings, Lausanne, 14–17 June 2010, vol. 5: pp. 411–418.
[9] S.G. Tesfahunegn, Ø. Ulleberg, P.J.S. Vie, T.M. Undeland, J. Power Sources 196 (2011) 10401–10414.
[10] L.T. Gibson, A.N. Kelly, Int. J. Hydrogen Energy 33 (2008) 5931–5940.
[11] B. Shabani, J. Andrews, S. Watkins, Solar Energy 84 (2010) 144–155.
[12] M.A.S. Masoum, H. Dehbonei, E.F. Fuchs, IEEE Trans. Energy Convers. 17 (2002) 514–522.
[13] M. Veerachary, T. Senjyu, K. Uezato, IEEE Trans. Aerosp. Electron. Syst. 38 (2002) 262–270.
[14] R. Chenni, M. Makhlouf, T. Kerbache, A. Bouzid, Energy 32 (2007) 1724–1730.
[15] S. Motahar, A.A. Alemrajabi, Int. J. Hydrogen Energy 34 (2009) 2396–2407.
[16] C.O. Colpan, I. Dincer, F. Hamdullahpur, Int. J. Energy Res. 32 (2007) 787–795.
[17] Residential Solar PV Power for Home Owners in Ontario. Web link: http://www.infinitekwh.com, (accessed 30.07.12.).
[18] Document #001-42023, 210 Solar Panel, SunPower Corporation. Web link: www.prevailingwindpower.com/sunpower.pdf, (accessed 26.06.12.).
[19] A.V. Virkar, SECA Core Technology Program Workshop (February 14, 2001). Atlanta.
[20] Weather Data, Department of Geography, University of Toronto Mississauga. Web link: http://www.utm.utoronto.ca/geography/resources/meteorological-station/weather-data, (accessed 26.06.12.).
[21] I. Knight, N. Kreutzer, M. Manning, M. Swinton, H. Ribberink, Energy Conversions in Buildings and Community System Programme, International Energy Agency, May 2007, Annex 42.